ELSEVIER

Advances in Water Resources 24 (2001) 105–117

Advances in Water Resources

www.elsevier.com/locate/advwatres

# In situ evaluation of solute retardation using single-well push–pull tests

M.H. Schroth [a,*], J.D. Istok [a], R. Haggerty [b]

[a] Department of Civil, Construction, and Environmental Engineering, 202 Apperson Hall, Oregon State University, Corvallis, OR 97331, USA
[b] Department of Geosciences, 104 Wilkinson Hall, Oregon State University, Corvallis, OR 97331, USA

**Abstract**

More efficient methods are needed for the in situ evaluation of solute sorption to aquifer sediments. The objective of this study was to develop a simplified method for estimating retardation factors for injected solutes from "push–pull" test extraction phase breakthrough curves (BTCs). Sensitivity analyses based on numerical simulations were used to evaluate the method performance for a variety of test conditions. Simulations were conducted for varying retardation factors, aquifer parameters and injection phase durations, for tests performed under nonideal transport conditions such as nonlinear equilibrium and linear nonequilibrium sorption, and for a test performed in a physically heterogeneous aquifer. Predicted retardation factors showed errors $\leqslant 14\%$ in tests performed under ideal transport conditions (physically homogeneous aquifer with spatially uniform dispersivity that does not vary from solute to solute, spatially uniform linear equilibrium sorption). The method performed more poorly for solutes with large retardation factors ($R > 20$) and for tests conducted under nonideal transport conditions, and is expected to perform poorly in aquifers with highly heterogeneous sorption. In an example application, we used the method to estimate the distribution coefficient for $^{85}Sr$ using data from a field test performed by Pickens JF, Jackson RE, Inch KJ, Merritt WF. (Water Resour Res 1981;17:529–44). Reasonable agreement was found between distribution coefficients obtained using the simplified method of estimation and those obtained by Pickens et al. (1981). 

*Keywords:* Solute transport; Sorption; Retardation; Nonuniform flow; Single-well test; Numerical simulation

## 1. Introduction

Quantitative information on sorption is needed to predict solute transport in the subsurface for applications to site characterization, risk assessment, and remedial design. The term sorption is used here to describe any reversible reaction between a solute (hereafter referred to as sorbing solute) and aquifer solids, e.g., due to ion exchange or adsorption/desorption reactions, that causes a reduced migration velocity and a delayed arrival time (retardation) for the sorbing solute relative to a conservative, i.e., a nonsorbing solute, hereafter referred to as tracer.

Sorption processes have been described by a variety of equilibrium and nonequilibrium models (e.g., [11,35]) containing one or more system specific parameters. Conventionally, these parameters have been obtained by small-scale laboratory batch and column studies performed with aquifer material collected from boreholes. However, it is not clear that sorption parameters obtained by laboratory studies are representative of in situ conditions (e.g., [14]). On the other hand, large-scale field transport experiments (e.g., [20,27,29]), which provide more representative values for sorption parameters than laboratory studies, are too time-consuming and expensive for routine use. For these reasons, fast and low-cost field methods for determining sorption parameters are needed.

Single-well injection–withdrawal tests, which we call "push–pull" tests, have been used for the quantitative determination of a wide range of aquifer physical, biological, and chemical characteristics. In a push–pull test, a prepared test solution containing one or more solutes is injected ("pushed") into the aquifer using an existing well; the test solution/groundwater mixture is then extracted ("pulled") from the same location. Aquifer characteristics are determined by an analysis of solute breakthrough curves (BTCs) obtained by measuring

* Corresponding author. Present address: Swiss Federal Institute of Technology (ETH), Zurich, Institute of Terrestrial Ecology, Grabenstr. 3, CH-8952 Schlieren, Switzerland. Tel.: +41-1-633-6039; fax: +41-1-633-1122.

*E-mail address:* schroth@ito.umnw.ethz.ch (M.H. Schroth).

0309-1708/01/$ - see front matter 
PII: S0309-1708(00)00023-3

solute concentrations at the well during the extraction phase.

Push–pull tracer tests have been used to study processes of advection and dispersion during nonuniform flow. A general form of the advection–dispersion equation for nonuniform radial flow was developed by Hoopes and Harleman [15] to study the displacement and mixing of groundwater by waste water injected into a single well. Type curves for the analysis of radial-flow fields were presented by Sauty [30]. Methods to estimate longitudinal dispersivity from push–pull tests were developed by Mercado [22] and Gelhar and Collins [6]. Pickens and Grisak [25] used push–pull tests to measure field-scale dispersion in a stratified aquifer. Based on the earlier work conducted by Leap and Kaplan [19], Hall et al. [13] derived equations to determine the effective porosity and regional groundwater velocity from push–pull test results. In addition, push–pull tests have proven useful as a diagnostic tool to quantify matrix diffusion in fractured rock (e.g., [10,21]).

Push–pull tests have also been used to quantify microbial metabolic activity including denitrification [33], petroleum hydrocarbon degradation [28], and aerobic respiration, denitrification, sulfate reduction, and methanogenesis [17,31]. Simplified methods for determining zero- and first-order reaction-rate coefficients from push–pull tests were recently developed by Haggerty et al. [12] and Snodgrass and Kitanidis [32].

Only a few studies have addressed the use of push–pull tests to characterize sorption of injected solutes to aquifer sediments. Drever and McKee [3] performed large-scale push–pull tests in an attempt to determine Langmuir isotherm sorption parameters for cations introduced during in situ coal gasification and uranium recovery. However, in their analysis, Drever and McKee [3] did not specifically take into account the radial-flow field in the vicinity of the injection/extraction well during the test. Instead sorption parameters were determined by matching the tails of extraction phase BTCs to type curves prepared by numerical simulation. Pickens et al. [26] performed push–pull tests to determine sediment–water distribution coefficients for $^{85}$Sr in a stratified aquifer. However, Pickens et al. [26] used only injection phase data from observation wells and did not attempt to estimate distribution coefficients from extraction phase BTCs.

The objective of this study was to develop a simplified method for estimating solute retardation factors for injected solutes from push–pull test BTCs. Sensitivity analyses were used to evaluate the method performance for a variety of simulated test conditions. Simulations were conducted for varying solute retardation factors, aquifer parameters and injection phase durations, for tests performed under nonideal transport conditions such as nonlinear equilibrium sorption and linear nonequilibrium sorption, and for a test performed in a physically heterogeneous confined aquifer. In an example application, we used the method to estimate the retardation factor and distribution coefficient for $^{85}$Sr using data from a field test performed by Pickens et al. [26].

## 2. Solute transport theory and simplified method development

The governing equation for one-dimensional solute transport subject to advection, dispersion and sorption during nonuniform, radial flow in a homogeneous, confined aquifer is (adopted from [1,34])

$$\frac{\partial C}{\partial t}+\frac{\rho_b}{n}\frac{\partial S}{\partial t}=\alpha_L|v|\frac{\partial^2 C}{\partial r^2}-v\frac{\partial C}{\partial r}, \tag{1}$$

where $C$ and $S$ are solute aqueous phase and solid (sorbed) phase concentrations, respectively, $\rho_b$ is bulk density, $n$ is effective porosity, $\alpha_L$ is longitudinal dispersivity, $t$ is time, $r$ is radial stance, and the average pore water velocity $v$ is

$$v=Q/2\pi bnr, \tag{2}$$

where $Q$ is the pumping rate (positive during the injection phase and negative during the extraction phase), and $b$ is aquifer thickness. Note that Eq. (2) assumes that the regional groundwater velocity is negligible compared to the imposed velocity due to pumping. Eq. (1) assumes that molecular diffusion is negligible and that mechanical dispersion is a linear function of $v$ (e.g., [1]).

Prior to solving Eq. (1), a sorption model must be specified. While a large number of such models are available (e.g., [35]), we restrict our analysis at this point to the linear equilibrium sorption isotherm

$$S=K_dC, \tag{3}$$

where $K_d$ is the distribution coefficient, which we assume to be spatially uniform. Additional information on the effects of the assumption of equilibrium sorption on transport in a radial-flow field is given in [34]. Substituting Eq. (3) into Eq. (1), the solute retardation factor $R$ can be defined as

$$R=1+\frac{\rho_b}{n}K_d. \tag{4}$$

Note that for a tracer $K_d=0$ and therefore $R=1$. Using Eq. (2), an "effective" velocity $v^*$ for a sorbing solute can be defined as

$$v^*=\frac{v}{R}=\frac{Q}{2\pi bnrR}. \tag{5}$$

During the injection phase of a push–pull test, a solute's frontal position $\hat{r}_{inj}$ (defined here as the location where $C/C_o=0.5$, where $C_o$ is the solute concentration in the

injected test solution) is obtained by rearranging and integrating Eq. (5)

$$\hat{r}_{\mathrm{inj}} = \sqrt{\frac{Q_{\mathrm{inj}} t_{\mathrm{inj}}}{\pi b n R} + r_{\mathrm{w}}^2}, \tag{6}$$

where $Q_{\mathrm{inj}}$ is the pumping rate during the injection phase, $t_{\mathrm{inj}}$ is the time since injection began, and $r_{\mathrm{w}}$ is the injection/extraction well radius. At the end of the injection phase, the frontal position attains a maximum value $\hat{r}_{\max}$ with

$$\hat{r}_{\max} = \sqrt{\frac{V_{\mathrm{inj}}}{\pi b n R} + r_{\mathrm{w}}^2} \tag{7}$$

with the total volume injected $V_{\mathrm{inj}} = Q_{\mathrm{inj}} T_{\mathrm{inj}}$, where $T_{\mathrm{inj}}$ is the duration of the injection phase.

During the extraction phase, flow is reversed and the frontal position $\hat{r}_{\mathrm{ext}}$ is given by

$$\hat{r}_{\mathrm{ext}} = \sqrt{\hat{r}_{\max}^2 + \frac{Q_{\mathrm{ext}} t_{\mathrm{ext}}}{\pi b n R}}, \tag{8}$$

where $Q_{\mathrm{ext}}$ is the pumping rate during the extraction phase (not necessarily equal in magnitude to $Q_{\mathrm{inj}}$) and $t_{\mathrm{ext}}$ is the time since extraction began. Note that Eq. (8) is only meaningful for $|Q_{\mathrm{ext}}| t_{\mathrm{ext}} \leqslant V_{\mathrm{inj}}$.

Eqs. (6)–(8) reveal the inverse quadratic variation in frontal position with time due to the radial-velocity field (Eqs. (2) and (5)). During the injection phase, a sorbing solute ($R > 1$) will travel at a smaller effective velocity (Eq. (5)) and penetrate a smaller radial distance into the aquifer (Eqs. (6) and (7)) than a tracer (Fig. 1(a)). Conversely, the difference in frontal positions for a sorbing solute and tracer will continuously decrease during the extraction phase (Eq. (8), Fig. 1(b)). Finally, when $|Q_{\mathrm{ext}}| t_{\mathrm{ext}} = V_{\mathrm{inj}}$, the frontal positions for the sorbing solute and tracer will coincide at $r = r_{\mathrm{w}}$. Thus, unlike in a well-to-well test in which the difference in arrival times for a sorbing solute and a tracer can be used to estimate a retardation factor, in a push–pull test, the arrival times of a sorbing solute and tracer during the extraction phase are identical and hence provide no information on the retardation factor of the injected sorbing solute. However, in the next section, we show that retardation factors can be estimated from extraction phase BTCs by considering dispersion.

### 2.1. Simplified method for estimating retardation factors from push–pull tests

In this section, we develop a simplified method for estimating solute retardation factors from push–pull tests based on a previously conducted analysis of longitudinal dispersion during radial flow [6].

Considering longitudinal dispersion only, Gelhar and Collins [6] derived approximate solutions to Eq. (1) with $S = 0$ by rewriting Eq. (1) in the form of a diffusion equation. Neglecting molecular diffusion, the approximate solution for tracer concentration during the injection phase of a push–pull test is (adopted from [6])

$$\frac{C}{C_{\mathrm{o}}} = \frac{1}{2}\operatorname{erfc}\left\{\left(r^2 - \hat{r}_{\mathrm{inj}}^2\right) \Big/ \left[\frac{16}{3}\alpha_{\mathrm{L}}\left(\hat{r}_{\mathrm{inj}}^3 - r_{\mathrm{w}}^3\right)\right]^{1/2}\right\}, \tag{9}$$

where $\hat{r}_{\mathrm{inj}}$ is given by Eq. (6).

During the subsequent extraction phase, the approximate solution for tracer concentration is given by

$$\frac{C}{C_{\mathrm{o}}} = \frac{1}{2}\operatorname{erfc}\left\{\left(r^2 - \hat{r}_{\mathrm{ext}}^2\right) \Big/ \left[\frac{16}{3}\alpha_{\mathrm{L}}\left(2\hat{r}_{\max}^3 - \hat{r}_{\mathrm{ext}}^3 - r_{\mathrm{w}}^3\right)\right]^{1/2}\right\}, \tag{10}$$

where $\hat{r}_{\max}$ and $\hat{r}_{\mathrm{ext}}$ are given by Eqs. (7) and (8), respectively. Furthermore, neglecting the well radius in Eq. (10), the approximate solution for tracer concentration at the injection/extraction well during the extraction phase is [6]

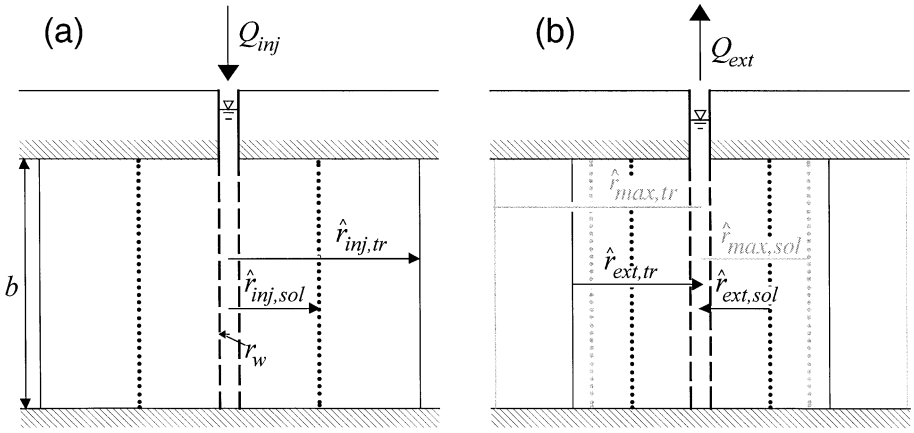


Fig. 1. Frontal positions ($C/C_{\mathrm{o}} = 0.5$) for a tracer (subscript "tr") and a co-injected sorbing solute (subscript "sol") during: (a) the injection phase and (b) prior to (gray lines and labels) and during the extraction phase of a push–pull test conducted under ideal transport conditions in a homogeneous confined aquifer.

$$\frac{C}{C_o} = \frac{1}{2}\operatorname{erfc}\left\{\left(\frac{V_{ext}}{V_{inj}} - 1\right)\Big/\left[\frac{16}{3}\frac{\alpha_L}{\hat{r}_{max}}\left(2 - \left|1 - \frac{V_{ext}}{V_{inj}}\right|^{1/2} \times \left(1 - \frac{V_{ext}}{V_{inj}}\right)\right)\right]^{1/2}\right\}, \quad (11)$$

where $V_{ext}$ is the cumulative extracted volume ($V_{ext} = |Q_{ext}|t_{ext}$) and $\hat{r}_{max}$ is given by Eq. (7) with $r_w = 0$. Eqs. (7) and (11) may be used to determine $\alpha_L$ from a push–pull test tracer BTC obtained at the injection/extraction well during the extraction phase of the test. First, the tracer frontal position at the end of the injection phase, $\hat{r}_{max,tr}$, is computed from Eq. (7) based on known values of $V_{inj}, b, n$ and $R = 1$. Then, Eq. (11) with $\hat{r}_{max} = \hat{r}_{max,tr}$ is fit to the tracer BTC to obtain an estimate for $\alpha_L$.

Under ideal transport conditions (physically homogeneous aquifer with spatially uniform dispersivity that does not vary from solute to solute, spatially uniform linear equilibrium sorption) the dispersivity is a property of the aquifer and should therefore be identical for a sorbing solute and a co-injected tracer. Differences in the shape of tracer and sorbing solute BTCs (Eq. (11)) may then be attributed to retardation of the sorbing solute relative to the tracer. Thus, we propose the following method for estimating retardation factors for a sorbing solute from push–pull test extraction phase BTCs: (1) determine $\hat{r}_{max,tr}$ from Eq. (7) and $\alpha_L$ from the tracer extraction phase BTC using Eq. (11); (2) keeping $\alpha_L$ fixed in Eq. (11), estimate the sorbing solute frontal position at the end of the injection phase $\hat{r}_{max,sol}$ by fitting Eq. (11) to the sorbing solute BTC; and (3) employing Eq. (7), an estimate of the retardation factor for the sorbing solute ($R^*$) can be obtained from

$$R^* = (\hat{r}_{max,tr}/\hat{r}_{max,sol})^2. \quad (12)$$

Note that this method does not require the use of a flow and transport model, and it can be easily implemented using a spreadsheet program. Nonetheless, other methods may be employed to estimate $R$ from push–pull test BTCs. For example, numerical solutions to Eq. (1) may be used to estimate $R$ from sorbing solute BTCs using inverse modeling.

## 3. Numerical methods

### 3.1. Overview

One- and two-dimensional simulations were conducted (1) to investigate the effects of varying retardation factors on BTCs obtained at the injection/extraction well during the extraction phase of a push–pull test, and (2) to evaluate the performance of the simplified method for estimating retardation factors for a variety of simulated test conditions. Simulations were performed using the Subsurface Transport Over Multiple Phases (STOMP) code [36]. STOMP is a fully implicit volume-integrated finite difference simulator for modeling one-, two-, and three-dimensional flow and transport, which has been extensively tested and validated against published analytical solutions as well as other numerical codes (e.g., [24]). For all simulations, the total variation diminishing scheme was employed [37], which consists of a third-order flux limiter permitting oscillation-free numerical solutions while minimizing numerical dispersion for a wide range of grid Peclet numbers [8]. An additional simulation for conditions of linear nonequilibrium sorption was performed using the STAMMT-R code [9], which solves transport and multirate mass-transfer equations for push–pull and well-to-well tracer tests. The solutions assume homogeneous media, but deal with a wide range of mass-transfer scenarios.

For all simulations, extraction phase BTCs were obtained by tracking tracer and sorbing solute fluxes at the injection/extraction well. BTCs were then analyzed to obtain estimates for retardation factors for the sorbing solutes and these were compared with the values of retardation factors used in the numerical simulations.

### 3.2. Simulations of tests conducted under ideal transport conditions

One-dimensional simulations of tests conducted under ideal transport conditions (confined aquifer with homogeneous physical and chemical properties; linear equilibrium sorption) were performed for a tracer and six sorbing solutes, for which values of $K_d$ were selected to give computed retardation factors ranging between 2 and 100 (Eq. (4)).

The computational domain consisted of a line of 250 nodes with a uniform node spacing of $\Delta r = 1.0$ cm. The time-step size during the simulations varied between 2 and 10 s. Initial conditions were a constant hydraulic head for the aqueous phase and $C = 0$ and $S = 0$ for all solutes. Time-varying third-type flux boundary conditions at $r_w = 252.5$ cm were used to represent pumping at the injection/extraction well; constant head and zero solute flux boundary conditions at $r = 252.5$ cm were used to represent aquifer conditions beyond the radius of influence of the well.

Simulations were conducted for a "base case" (BC) and a set of six additional cases, which had values of a single parameter ($\alpha_L, n$ or $T_{inj}$) larger or smaller than in the BC. BC parameters ($\alpha_L = 1.0$ cm, $n = 0.35$, $T_{inj} = 12$ h, $b = 20$ cm, $vn = \pm 0.83$ cm/min at $r = r_w$) were chosen to represent a typical test conducted in an unconsolidated sand. The duration of the injection phase was selected to give $\hat{r}_{max} \approx 93$ cm for the tracer. Values

for $\alpha_L$ similar to the BC value of 1.0 cm were observed previously in laboratory experiments conducted over similar length scales with a sandy loam [16]. For the additional cases, $\alpha_L$ was varied from 0.1 to 10 cm, $n$ was varied from 0.25 to 0.45, and $T_{inj}$ was varied from 6 to 24 h, while $vn$ and $b$ were identical for all simulations during both injection and extraction phases.

### 3.3. Simulations of tests conducted under nonideal transport conditions

One-dimensional simulations were performed for tests conducted under conditions of nonlinear equilibrium sorption and linear nonequilibrium sorption. In addition, a two-dimensional simulation was performed for a test conducted in a physically heterogeneous confined aquifer.

For the simulation of a test conducted under conditions of nonlinear equilibrium sorption, we substituted the sorption term in Eq. (1) with the Langmuir sorption isotherm (e.g., see [4])

$$S = \frac{S_{max} K_L C}{1 + K_L C}, \tag{13}$$

where $S_{max}$ is the maximum sorption capacity, and $K_L$ is the Langmuir coefficient. Note that for $C \ll 1/K_L$, $S = S_{max} K_L C$, which represents the linear sorption isotherm (Eq. (3)) with $K_d = S_{max} K_L$. The simulation was performed for a tracer, a solute subject to linear sorption ($R = 10$), and five additional solutes subject to Langmuir-type sorption, for which $S_{max} K_L$ was identical to that of the linearly sorbing solute. Variation in the sorption behavior of solutes subject to Langmuir-type sorption was introduced by varying the solutes' $C_o$, thus altering $C$ in Eq. (13). When expressed in terms of a dimensionless number, $\bar{C}_0$, with $\bar{C}_0 = C_o K_L$, values employed were in the range of $0.5 \leqslant \bar{C}_0 \leqslant 500$. The computational domain, as well as initial and boundary conditions for this simulation were identical to those described in Section 3.2.

For the simulation of a test conducted under conditions of linear nonequilibrium sorption, we substituted the sorption term in Eq. (1) with the first-order chemical nonequilibrium model (e.g., see [11,34])

$$\frac{\partial S}{\partial t} = k(K_d C - S), \tag{14}$$

where $k$ is the first-order rate coefficient, which may be expressed in dimensionless form as $\bar{k} = k 2\pi b n \alpha_L^2 / Q$ [34]. The simulation was performed for a tracer, a solute subject to linear equilibrium sorption ($R = 10$), and five additional solutes subject to nonequilibrium sorption. Values of $K_d$ were identical for all sorbing solutes. Variation in the sorption behavior of solutes subject to nonequilibrium sorption was introduced by varying $\bar{k}$ in the range of $10^{-1} \leqslant \bar{k} \leqslant 10^{-6}$. This simulation was performed using the STAMMT-R code with the computational domain, initial and boundary conditions identical to those described in Section 3.2.

For the simulation of a test conducted across the entire saturated thickness of a heterogeneous confined aquifer, the two-dimensional computational domain consisted of an array of 1200 nodes distributed in a radial ($r$)–vertical ($z$) coordinate system (where $z$ is the vertical distance from the base of the aquifer). We used a variable node spacing of $\Delta r = 5$ cm for $0 \text{ cm} < (r - r_w) < 50$ cm, $\Delta r = 10$ cm for $50 \text{ cm} < (r - r_w) < 200$ cm, $\Delta r = 20$ cm for $200 \text{ cm} < (r - r_w) < 300$ cm, and a uniform node spacing of $\Delta z = 5$ cm for $0 \text{ cm} \leqslant z \leqslant 200$ cm. The domain was assumed to contain layers and lenses of three different isotropic porous media with $\alpha_L = 1.0$ cm and $\alpha_T = 0.05$ cm for all media. Layers of medium 1 ($n = 0.35$, hydraulic conductivity $K = 4.33$ cm/min) and medium 2 ($n = 0.40$, $K = 0.35$ cm/min) were placed into the domain at random, followed by randomly replacing areas within layers of medium 1 and 2 with 15 lenses of medium 3 ($n = 0.45$, $K = 0.0035$ cm/min) (see Fig. 5(a) in Section 4). The simulation time step size varied between 2 and 10 s. Initial conditions were a constant hydraulic head for the aqueous phase and $C = 0$ and $S = 0$ for all solutes. Time-varying first-type (Dirichlet) boundary conditions (resulting in $vn = \pm 0.83$ cm/min at $r = r_w$, averaged across the entire thickness), together with time-varying third-type solute flux boundary conditions were used at $r_w = 2.5$ cm to represent pumping at the injection/extraction well. Zero flux boundary conditions were imposed along the aquifer base ($z = 0$ cm) and top ($z = 200$ cm); constant head and zero solute flux boundary conditions at $r = 302.5$ cm were used to represent aquifer conditions beyond the radius of influence of the well. The injection/extraction of a tracer and six sorbing solutes ($2 \leqslant R \leqslant 100$) was simulated along $0 \text{ cm} < z < 200$ cm for $T_{inj} = 12$ h. Test conditions for this simulation were selected such that $\hat{r}_{max,tr} \leqslant 150$ cm in any medium.

## 4. Results and discussion

### 4.1. Simulations of tests conducted under ideal transport conditions

Extraction phase BTCs for the BC simulation of a test in a physically and chemically homogeneous confined aquifer with sorbing solutes subject to linear equilibrium sorption showed an almost simultaneous arrival of the frontal positions ($C/C_o = 0.5$) for all solutes near $V_{ext}/V_{inj} = 1.0$ (Fig. 2), as predicted by Eq. (8). However, no perfect coincidence of the BTCs was obtained at $C/C_o = 0.5$ and $V_{ext}/V_{inj} = 1.0$, as e.g., predicted by Eq. (11), due to the variable dispersion in

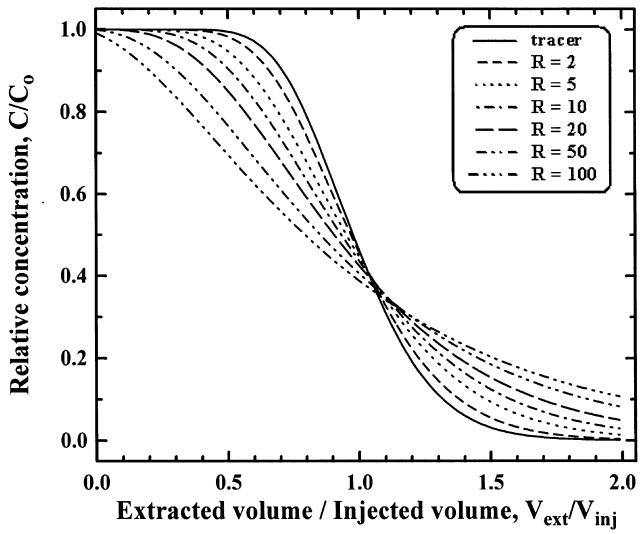


Fig. 2. Simulated breakthrough curves for a tracer and co-injected sorbing solutes ($2 \leqslant R \leqslant 100$) obtained at the injection/extraction well during the extraction phase of a push–pull test conducted under ideal transport conditions using BC parameters.

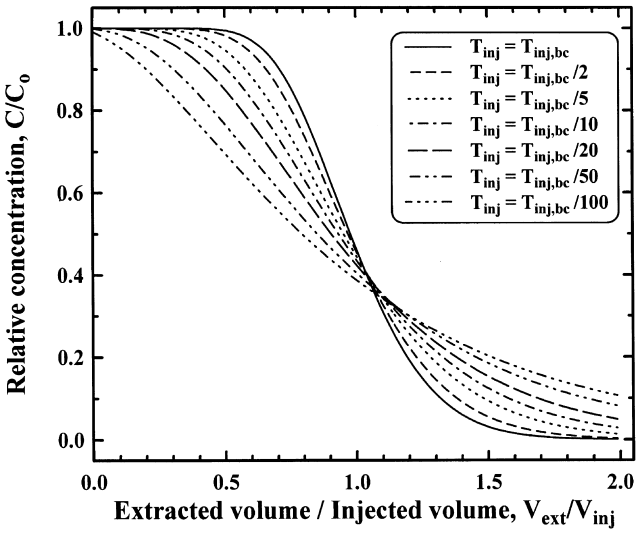


Fig. 3. Simulated tracer breakthrough curves obtained at the injection/extraction well during the extraction phase of multiple push–pull tests conducted under ideal transport conditions for varying total injection times $T_{\text{inj}}$, shown as fractions of the total injection time for the BC simulation $T_{\text{inj,bc}}$.

the nonlinear flow field. Similar results were obtained for all simulations conducted in a homogeneous confined aquifer (not shown), verifying that differences in arrival times do not provide sufficient information to estimate retardation factors.

However, BTCs for solutes with increasing retardation factors showed an increasing width of their dispersed fronts (Fig. 2). The width of the dispersed front can be defined as the increment $\Delta(V_{\text{ext}}/V_{\text{inj}})$ between the intercepts of the tangent line at $C/C_{\text{o}} = 0.5$ with horizontal lines at $C/C_{\text{o}} = 1.0$ and 0.0 [22]. This observation is in agreement with our analysis of extraction phase BTCs for sorbing solutes during radial flow based on the theory developed by Gelhar and Collins [6], where changes in the shape of the BTCs (Eq. (11)) are expected as a function of $R^{1/2}$ (Eq. (7)).

A set of BTCs identical to those presented in Fig. 2 was obtained from multiple simulations of tracer push–pull tests using the same parameter set as for the BC simulation except for $T_{\text{inj}}$, which was varied in fractions of the duration of the injection phase of the BC simulation $T_{\text{inj,bc}}$ (Fig. 3). Note that the fractions of $T_{\text{inj,bc}}$ used to generate Fig. 3 (2–100) are identical to retardation factors chosen for the BC simulation (Fig. 2). Therefore, Fig. 3 displays the extraction phase BTCs for tracers that were pushed to the same value of $\hat{r}_{\max}$ as the corresponding sorbing solutes in Fig. 2 (Eq. (7)). Thus, the amount of variable dispersion during transport for a tracer is identical to that of a sorbing solute with identical $\hat{r}_{\max}$. This may be explained as follows. If Eqs. (2) and (3) are inserted into Eq. (1), and we divide the right-hand side of Eq. (1) by $R$, then the hydrodynamic dispersion coefficient becomes $\alpha_{\text{L}}|v|/R$, thus indicating a smaller dispersion coefficient for a sorbing solute than for a tracer. However, dispersion will act upon a sorbing solute $R$ times longer than on the corresponding tracer, since the arrival time of a sorbing solute $\hat{t}_{\text{sol}}$ at any location along the flow path is related to that of a tracer $\hat{t}_{\text{tr}}$ at that location by $\hat{t}_{\text{sol}}/\hat{t}_{\text{tr}} = R$. Thus, prolonged dispersion will exactly offset the reduction in the dispersion coefficient for a sorbing solute. Note that this statement also applies to flow in a uniform flow field and that it is only valid under ideal transport conditions, as defined earlier.

Using BC parameters in Eq. (7), we computed $\hat{r}_{\max,\text{tr}} = 92.9$ cm, and we obtained $\alpha_{\text{L}} = 0.98$ cm by fitting Eq. (11) to the tracer BTC (Fig. 2). The fitted value of $\alpha_{\text{L}}$ is in good agreement with the simulated value of $\alpha_{\text{L}} = 1.0$ cm. Similar results were obtained for simulations in which $n$ and $T_{\text{inj}}$ were varied, with estimates for $\alpha_{\text{L}}$ ranging between 0.97 and 0.99. Using the simplified method of estimation for radial flow, we obtained estimates of $\hat{r}_{\max}$ and predicted retardation factors $R^*$ for all solutes during simulations of push–pull tests under ideal transport conditions (Table 1). Differences $\leqslant 14\%$ between values of $R$ and $R^*$ were observed for all solutes for the BC simulation as well as for simulations in which $n$ and $T_{\text{inj}}$ were varied.

In general, differences between $R$ and $R^*$ increased with increasing $R$ (Table 1). This may be explained by considering the mean-squared error (MSE) between simulated and fitted (Eq. (11)) BTCs, which also increased with increasing $R$ (not shown). For example, for the BC simulation, the MSE between fitted and simulated tracer BTC was $1.66 \times 10^{-4}$, and the MSE increased monotonically to $5.64 \times 10^{-3}$ for the fit of the

Table 1
Best fit values of frontal positions at the end of the injection phase ($\hat{r}_{max}$) and estimated solute retardation factors ($R^*$) for solutes in simulations of push–pull tests conducted under ideal transport conditions[a]

| Simulation | BC | | Low $n$ (0.25) | | High $n$ (0.45) | | Low $T_{inj}$ (6 h) | | High $T_{inj}$ (24 h) | | Low $\alpha_L$ (0.1 cm) | | High $\alpha_L$ (10 cm) | | BC, guess $n = 0.25$ | | BC, guess $n = 0.45$ | |
|---|---|---|---|---|---|---|---|---|---|---|---|---|---|---|---|---|---|---|
| Simulated $R$ | $\hat{r}_{max}$ (cm) | $R^*$ | $\hat{r}_{max}$ (cm) | $R^*$ | $\hat{r}_{max}$ (cm) | $R^*$ | $\hat{r}_{max}$ (cm) | $R^*$ | $\hat{r}_{max}$ (cm) | $R^*$ | $\hat{r}_{max}$ (cm) | $R^*$ | $\hat{r}_{max}$ (cm) | $R^*$ | $\hat{r}_{max}$ (cm) | $R^*$ | $\hat{r}_{max}$ (cm) | $R^*$ |
| Tracer[b] | 92.9 | 1.00 | 110 | 1.00 | 81.9 | 1.00 | 65.7 | 1.00 | 131 | 1.00 | 92.9 | 1.00 | 92.9 | 1.00 | 110 | 1.00 | 81.9 | 1.00 |
| 2 | 65.9 | 1.99 | 77.9 | 1.99 | 58.2 | 1.98 | 46.7 | 1.98 | 93.1 | 1.99 | 64.0 | 2.11 | 67.2 | 1.91 | 78.0 | 1.99 | 58.2 | 1.98 |
| 5 | 42.2 | 4.85 | 49.7 | 4.89 | 37.3 | 4.82 | 30.1 | 4.76 | 59.3 | 4.91 | 39.5 | 5.53 | 42.3 | 4.82 | 49.9 | 4.85 | 37.2 | 4.85 |
| 10 | 30.3 | 9.40 | 35.6 | 9.53 | 26.8 | 9.34 | 21.6 | 9.25 | 42.4 | 9.60 | 27.5 | 11.4 | 28.4 | 10.7 | 35.8 | 9.42 | 26.7 | 9.41 |
| 20 | 21.8 | 18.2 | 25.6 | 18.4 | 19.3 | 18.0 | 15.5 | 18.0 | 30.4 | 18.7 | 19.2 | 23.4 | 17.9 | 26.9 | 25.8 | 18.1 | 19.2 | 18.2 |
| 50 | 14.0 | 44.0 | 16.5 | 44.4 | 12.4 | 43.6 | 9.71 | 45.8 | 19.7 | 44.5 | 11.8 | 61.9 | 8.57 | 117 | 16.6 | 43.8 | 12.4 | 43.6 |
| 100 | 9.79 | 90.0 | 11.7 | 88.2 | 8.51 | 92.6 | 6.43 | 104 | 14.1 | 86.4 | 8.02 | 135 | 4.21 | 487 | 11.6 | 89.8 | 8.63 | 90.1 |

[a] Values of $R^*$ were obtained using the simplified method of estimation. BC simulation parameters were $\alpha_L = 1.0$ cm, $n = 0.35$, and $T_{inj} = 12$ h.
[b] Values of $\hat{r}_{max,tr}$ were computed using Eq. (7).

$R = 100$ BTC. This phenomenon is due to the fact that Eqs. (9)–(11) are *approximate* solutions. As specified by Gelhar and Collins [6], these approximate solutions are only accurate if $(\alpha_L/L_o)^{1/2} \ll 1$, where $L_o$ is the total distance traveled by the solute front. In other words, a higher accuracy is achieved when the solute dispersed zone width is small compared to $L_o$. However, $L_o$ decreased as a function of $R$ (note that for a push–pull test $L_o = 2\hat{r}_{max}$, Eq. (7)). Thus, less accurate fits of Eq. (11) to BTCs are expected for solutes with larger values of $R$.

The foregoing analysis is particularly relevant to simulations in which $\alpha_L$ was varied (Table 1). For the case of $\alpha_L = 10$ cm, reasonably accurate predictions of retardation factors were obtained only for solutes with $R \leqslant 20$. Differences between $R$ and $R^*$ dramatically increased for sorbing solutes with $R > 20$ because the assumption of $(\alpha_L/L_o)^{1/2} \ll 1$ was increasingly violated. For example, we computed $(\alpha_L/L_o)^{1/2} = 1.09$ for the solute with $R = 100$, and the poor agreement between the simulated and the fitted BTC was reflected in a MSE value of $7.51 \times 10^{-2}$.

To corroborate this line of reasoning, we conducted an additional simulation in which $T_{inj}$ was increased by a factor of 10. For this simulation, the numerical domain was extended to a total length of 7.5 m. In case of the solute with $R = 100$, we found $R^* = 85.9$ with a MSE of $2.49 \times 10^{-2}$. Thus, for solutes with larger values of $R$, larger values of $L_o$ and therefore $\hat{r}_{max}$ (i.e., a longer injection phase duration or higher injection rate) are required to more closely satisfy $(\alpha_L/L_o)^{1/2} \ll 1$, and hence to improve the agreement between $R$ and $R^*$.

Larger discrepancies between $R$ and $R^*$ compared to the BC were also observed in simulations with $\alpha_L = 0.1$ cm for solutes with larger values of $R$ (Table 1). Causes for these discrepancies remain uncertain, as small values of MSE ranging between $4.75 \times 10^{-6}$ and $1.66 \times 10^{-4}$ indicated good agreement between simulated and fitted BTCs. A possible explanation is that numerical dispersion may have been more important in these simulations due to the small value of $\alpha_L$.

So far, we assumed complete knowledge of parameter values required in the computation of $\hat{r}_{max}$ (Eq. (7)). However, the effective porosity $n$ in particular is usually not known precisely. Similarly, the aquifer thickness $b$ may be uncertain. We investigated the effect of uncertainty in $n$ or $b$ on the method performance by reanalyzing the BC simulation using values of $n$ that were both lower (0.25) and higher (0.45) than the actual simulated value (0.35, Table 1). (Note that changing $n$ or $b$ has an equivalent effect on $\hat{r}_{max}$ (Eq. (7)).) Interestingly, results almost identical to the original BC analysis were obtained for both low and high values of $n$. Differences $\leqslant 13\%$ between $R$ and $R^*$ were found for all values of $R$, and MSE values were similar to those in the BC analysis (not shown). The relative insensitivity of the method to initial guesses of $n$ may be explained as follows. Predicted values of $\hat{r}_{max}$ for tracer and sorbing solutes are equally affected by uncertainties in $n$ (and would be equally affected by uncertainties in $b$). Therefore, using the ratio of $\hat{r}_{max,tr}$ and $\hat{r}_{max,sol}$ to estimate retardation factors (Eq. (12)) effectively cancels out effects of uncertainties in $n$ or $b$.

### 4.2. Simulations of tests conducted under nonideal transport conditions

Extraction phase BTCs for the simulation of a test conducted under conditions of nonlinear equilibrium sorption (Fig. 4) were different from those obtained under conditions of linear equilibrium sorption (Fig. 2). Increasing $\bar{C}_0$ in Fig. 4 enhanced differences in BTCs between solutes subject to Langmuir-type sorption and the linearly sorbing solute ($R = 10$). As a result of increasing $\bar{C}_0$, $C$ also increased during the test and the sorption behavior gradually shifted from the linear sorption branch of the Langmuir isotherm ($S = S_{max}K_L C$ for $C \ll 1/K_L$) to the branch where sorption is limited by the number of sorption sites ($S = S_{max}$ for $C \gg 1/K_L$). The most extreme case for this behavior is the BTC of the sorbing solute with $\bar{C}_0 = 500$, which closely matched the tracer BTC in Fig. 4, indicating almost conservative transport of the sorbing solute. Perhaps the most obvious visual difference in Fig. 4 compared to Fig. 2 is that sorbing solute BTCs in Fig. 4 do not all coincide near $V_{ext}/V_{inj} = 1$. Rather, the location where sorbing solute BTCs cross the tracer BTC shifted gradually toward significantly larger values

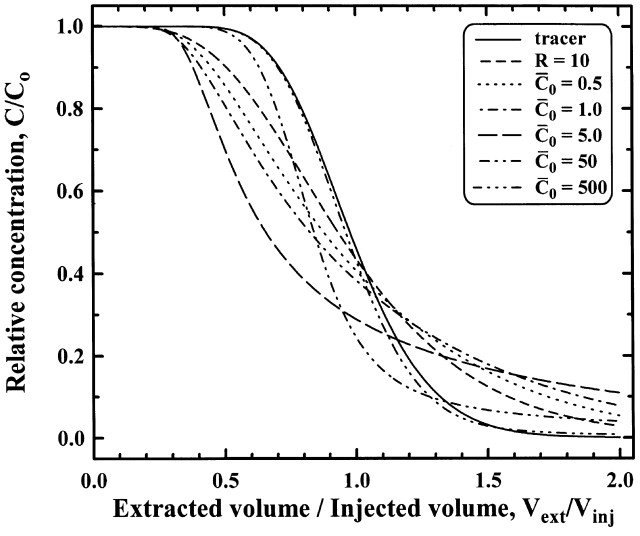


Fig. 4. Simulated breakthrough curves for a tracer, a solute subject to linear equilibrium sorption ($R = 10$), and five solutes subject to nonlinear (Langmuir-type) equilibrium sorption obtained at the injection/extraction well during the extraction phase of a push–pull test. Variations in the sorption behavior of solutes subject to nonlinear sorption was introduced by varying the solutes' injection concentration, displayed here in dimensionless form as $\bar{C}_0$.

of $V_{ext}/V_{inj}$. For example, for the sorbing solute with $\bar{C}_0 = 500$, that location was near $V_{ext}/V_{inj} = 1.5$. This phenomenon may serve as a qualitative indicator of nonideal transport conditions during a push–pull test.

As a consequence of the differences in the shape of BTCs obtained in Fig. 4, values of $R^*$ initially increased for solutes subject to Langmuir-type sorption ($0.5 \leqslant \bar{C}_0 \leqslant 5.0$) (Table 2). This is in disagreement with predicted Langmuir retardation factors, $R_L$, given as (e.g., [4])

$$R_L = 1 + \frac{\rho_b}{n}\left(\frac{S_{max}K_L}{(1+K_L C)^2}\right), \tag{15}$$

which should monotonically decrease with increasing $\bar{C}_0$ and, hence, increasing $C$. In our simulation, this is true only for sorbing solutes with $50 \leqslant \bar{C}_0 \leqslant 500$. In addition, agreement between simulated and fitted (Eq. (11)) BTCs was increasingly poor for sorbing solutes with $0.5 \leqslant \bar{C}_0 \leqslant 50$, as witnessed by increasing MSR values (Table 2). Thus, our simplified method for estimating $R$ appears not be generally applicable to cases of nonlinear equilibrium solute sorption. For cases in which Langmuir-type sorption is suspected during a push–pull test, we therefore refer the reader to Drever and McKee [3], who have developed a method for estimating $R_L$ from push–pull tests by matching tails of extraction phase BTCs to type curves. Moreover, performing multiple push–pull tests with varying $\bar{C}_0$ may help assess the presence of nonlinear sorption conditions.

Extraction phase BTCs for the simulation of a test conducted under conditions of linear nonequilibrium sorption (Fig. 5) also differed from those obtained under conditions of linear equilibrium sorption (Fig. 2). In Fig. 5, increasing nonequilibrium conditions were simulated using decreasing values of $\bar{k}$. Note that $\bar{k}$ represents a Damkohler number, expressing the rate of mass transfer relative to the rate of advection. Decreasing $\bar{k}$ generally enhanced differences in BTCs between solutes subject to nonequilibrium sorption and the solute subject to equilibrium sorption ($R = 10$). For the smallest value of

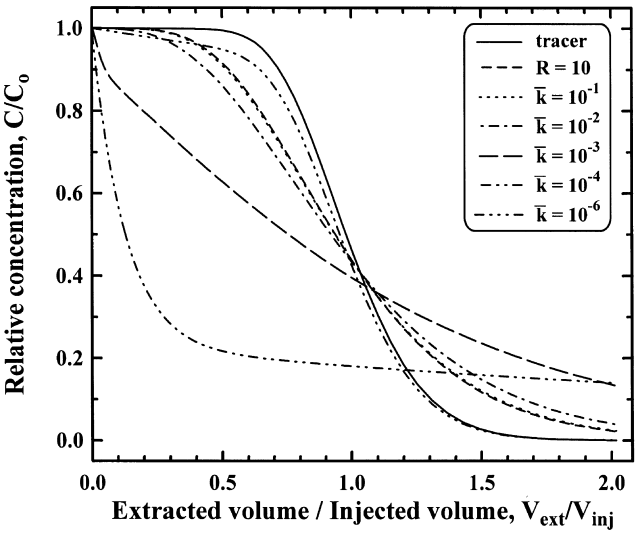


Fig. 5. Simulated breakthrough curves for a tracer, a solute subject to linear equilibrium sorption ($R = 10$), and five solutes subject to linear nonequilibrium sorption obtained at the injection/extraction well during the extraction phase of a push–pull test. Variations in the sorption behavior of solutes subject to nonequilibrium sorption was introduced by varying the solutes' first-order rate coefficient, displayed in dimensionless form as $\bar{k}$.

$\bar{k}$ ($10^{-6}$), the BTC of the respective sorbing solute approached that of the tracer, indicating that sorption was almost completely blocked, i.e., $\partial S/\partial t$ approached zero in Eq. (14). Similar to the case of nonlinear equilibrium sorption (Fig. 4), sorbing solute BTCs in Fig. 5 did not all coincide near $V_{ext}/V_{inj} = 1$, but the location where sorbing solute BTCs crossed the tracer BTC shifted gradually toward significantly larger values of $V_{ext}/V_{inj}$. Again, this phenomenon may serve as a qualitative indicator of nonideal transport conditions (here nonequilibrium conditions) during a push–pull test.

As a consequence of the shape of BTCs obtained in Fig. 5, values of $R^*$ generally increased with decreasing $\bar{k}$ (Table 2). A reasonable value of $R^*$ (1.92) was obtained only for the solute with $\bar{k} = 10^{-6}$. Increasing disagreement between simulated and fitted (Eq. (11)) BTCs for

Table 2
Estimated solute retardation factors ($R^*$) and MSR between simulated and fitted breakthrough curves in simulations for push–pull tests conducted under nonideal transport conditions of nonlinear equilibrium sorption, linear nonequilibrium sorption, and a test conducted in a physically heterogeneous aquifer[a]

| Nonlinear sorption | | | Nonequilibrium sorption | | | Heterogeneous aquifer | | |
|---|---|---|---|---|---|---|---|---|
| Solute | $R^*$ | MSR | Solute | $R^*$ | MSR | Solute | $R^*$ | MSR |
| Tracer | 1.00 | $1.65 \times 10^{-4}$ | Tracer | 1.00 | $2.59 \times 10^{-5}$ | Tracer | 1.00 | $6.34 \times 10^{-3}$ |
| $R = 10$ | 9.40 | $9.42 \times 10^{-4}$ | $R = 10$ | 9.90 | $1.55 \times 10^{-4}$ | $R = 2$ | 0.79 | $4.13 \times 10^{-3}$ |
| $\bar{C}_0$[b] $= 0.5$ | 19.4 | $2.44 \times 10^{-3}$ | $\bar{k}$[c] $= 10^{-1}$ | 10.7 | $1.61 \times 10^{-4}$ | $R = 5$ | 0.91 | $3.07 \times 10^{-3}$ |
| $\bar{C}_0 = 1.0$ | 31.2 | $4.41 \times 10^{-3}$ | $\bar{k} = 10^{-2}$ | 20.1 | $2.29 \times 10^{-4}$ | $R = 10$ | 1.16 | $2.58 \times 10^{-3}$ |
| $\bar{C}_0 = 5.0$ | 54.7 | $1.74 \times 10^{-2}$ | $\bar{k} = 10^{-3}$ | 184 | $3.46 \times 10^{-4}$ | $R = 20$ | 2.06 | $2.88 \times 10^{-3}$ |
| $\bar{C}_0 = 50$ | 2.74 | $1.13 \times 10^{-2}$ | $\bar{k} = 10^{-4}$ | 985 | $4.60 \times 10^{-2}$ | $R = 50$ | 5.77 | $5.20 \times 10^{-3}$ |
| $\bar{C}_0 = 500$ | 0.86 | $6.90 \times 10^{-4}$ | $\bar{k} = 10^{-6}$ | 1.92 | $2.81 \times 10^{-4}$ | $R = 100$ | 14.5 | $9.18 \times 10^{-3}$ |

[a] Values of $R^*$ were obtained using the simplified method of estimation.
[b] Dimensionless injection concentration.
[c] Dimensionless first-order rate coefficient.

sorbing solutes with decreasing $\bar{k}$ was again witnessed by increasing MSR values relative to that of the tracer (Table 2). Thus, similar to the case of nonlinear equilibrium sorption, our simplified method for estimating $R$ appears not be generally applicable to cases of linear nonequilibrium sorption. However, nonequilibrium sorption effects during push–pull tests may be discerned by examining late-time concentrations, and they are particularly obvious in a double-logarithmic plot of the extraction phase BTCs [10,21]. Furthermore, performing multiple push–pull tests with varying $\bar{k}$ may help assess the presence of nonequilibrium sorption conditions.

Preferential flow of injected solutes was observed in aquifer layers containing the medium with the highest hydraulic conductivity in simulations conducted for the case when the injection/extraction was performed across the entire saturated thickness of a physically heterogeneous confined aquifer (Fig. 6(a)). Extreme differences in $\hat{r}_{\max}$ existed between solutes of different $R$ in different layers. For example, a value of $\hat{r}_{\max,\mathrm{tr}} \approx 145$ cm was observed in medium 1, whereas $\hat{r}_{\max,\mathrm{sol}}$ was $\approx 0$ for $R = 100$ in the medium 3 lens located in the upper-left corner of the computational domain.

Consequently, extraction phase BTCs for simulations conducted in a heterogeneous confined aquifer (Fig. 6(b)) were substantially different from those conducted in a homogeneous aquifer (Fig. 2). For the simulation conducted in a heterogeneous aquifer, the width of the dispersed zone did not increase monotonically for all solutes with increasing $R$, although a general trend of larger dispersed widths for solutes with larger values of R was observed (Fig. 6(b)). In particular, the tracer BTC showed multiple crossovers with BTCs of sorbing solutes (with $R \leqslant 20$) both prior to and after $V_{\mathrm{ext}}/V_{\mathrm{inj}} = 1.0$. The estimated value of $\alpha_{\mathrm{L}}$ (assuming an average $n = 0.40$ in Eq. (7)) was 2.96 cm, which was significantly different from the simulated value of $\alpha_{\mathrm{L}} = 1.0$ cm, reflecting the increased amount of dispersion due to velocity differences between the layers (e.g., [5]). The distorted shape of the tracer BTC led to poor agreement between simulated and fitted (Eq. (11)) BTCs (Table 2). In particular, the MSE for the tracer BTC ($6.34 \times 10^{-3}$) was larger than for all other solutes except for $R = 100$. This is a result of the increased heterogeneity encountered by the tracer, which subsequently led to unreasonably small predicted retardation factors $R^*$ (Table 2).

In this context, it is useful to consider the effects of macrodispersion during a push–pull test in somewhat greater detail. In their review paper, Gelhar et al. [7] classified the push–pull test as a tool with low reliability with respect to determining $\alpha_{\mathrm{L}}$ in the field. The authors argued that macrodispersion in a layered heterogeneous aquifer should be at least partially reversible during a push–pull test due to the reversal of the flow direction between the injection and extraction phase. This could

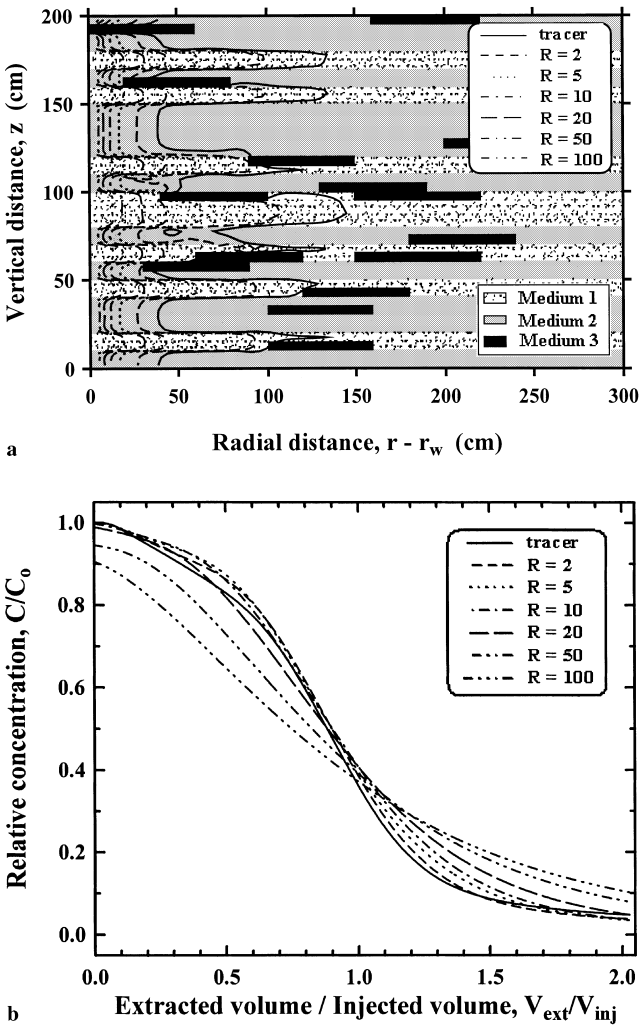


Fig. 6. Simulated push–pull test for a tracer and co-injected sorbing solutes ($2 \leqslant R \leqslant 100$) conducted in a heterogeneous confined aquifer: (a) frontal positions at the end of the injection phase (stipples, gray and black shading represent zones of different material properties) and (b) breakthrough curves obtained at the injection/extraction well during the extraction phase.

lead to a possible underprediction of $\alpha_{\mathrm{L}}$ using Eq. (11). To investigate this phenomenon in our simulation, we obtained the tracer injection phase BTC by tracking solute and water fluxes across the vertical axis at $(r - r_{\mathrm{w}}) = 80$ cm (Fig. 6(a)). Using Eq. (9), we obtained an estimate of $\alpha_{\mathrm{L}}$ (9.83 cm) that was much larger than the estimate of $\alpha_{\mathrm{L}}$ obtained from the tracer extraction phase BTC (2.96 cm), thus corroborating the argument of Gelhar et al. [7].

The performance of the simplified method of estimation is clearly discouraging for the simulation of a push–pull test conducted in a heterogeneous aquifer (Fig. 6). However, we note that this simulation was (for illustration purposes) conducted in an aquifer that was perfectly layered in the main flow direction, thus causing a significant amount of macrodispersion over a

relatively small solute travel distance. Certainly, if tests were conducted in an aquifer with a more random distribution of hydraulic conductivity (e.g., [12]), where local differences in $\hat{r}_{max}$ for any one solute were less extreme than in Fig. 6(a), then we would expect a better method performance.

It is also important to note that correlated sorption and hydraulic conductivity fields are responsible for the field-scale effect of macrokinetics (e.g., [2,23]). With macrokinetics, higher "effective" dispersivities are generally observed for sorbing solutes than for conservative tracers. Additionally, there is some indication that dispersivity is a function of sorption, at least at the pore scale (e.g., [18]). If either of these two conditions exist, it may limit the applicability of our method to estimate $R$. In our method, differences in the shape of tracer and sorbing solute BTCs are attributed to differences in the retardation factor rather than to effective dispersivities caused by macrokinetics or sorption-enhanced dispersion. No analysis is presented here to determine the effects of macrokinetics or sorption-enhanced dispersion on the accuracy of our method to estimate $R$.

### 4.3. Example field application

Pickens et al. [26] conducted a push–pull test to quantify the sorption of $^{85}$Sr in a sandy aquifer using $^{131}$I as a tracer. The aquifer was composed of several horizontal layers and the test was conducted in an ~8 m thick layer (confined below by a silty clay bed of ~1 m thickness and above by ~17 cm of silt and clay) consisting of well sorted very fine-to fine-grained sand. Sand porosities varied between 0.33 and 0.44 with an average value of 0.38, and the bulk density was calculated to be 1.7 g/cm$^3$. The injection/extraction well was constructed of 10.4 cm diameter PVC pipe and screened across almost the entire thickness of the selected aquifer layer. A total volume of $V_{inj} = 244$ m$^3$ of test solution containing $^{131}$I and $^{85}$Sr was injected over a period of $T_{inj} = 94.32$ h at a constant flow rate $Q_{inj} = 2.587$ m$^3$/h, resulting in an average $\hat{r}_{max,tr}$ of ~5.0 m. Extraction pumping began immediately following the injection phase at $Q_{ext} = 2.282$ m$^3$/h for 405.6 h (equivalent to $V_{ext}/V_{inj} = 3.6$). During the injection phase, water samples were collected from several depths using three multilevel samplers installed at radial distances of 0.36, 0.66 and 2.06 m from the injection/extraction well; during the extraction phase, water samples were collected from the injection/extraction well discharge line.

Distribution coefficients ($K_d$) for $^{85}$Sr, obtained from injection phase BTCs at three separate depth intervals, ranged from 2.6 to 4.5 ml/g [26]. These values were in good general agreement with values determined from sediment core analyses (4.3 ml/g $\leqslant K_d \leqslant$ 7.9 ml/g) and batch experiments (2.8 ml/g $\leqslant K_d \leqslant$ 7.8 ml/g). While extraction phase BTCs for $^{131}$I and $^{85}$Sr were presented (Fig. 7), Pickens et al. [26] did not report a quantitative analysis and considered the increase in width of the dispersed front for the $^{85}$Sr BTC compared to the $^{131}$I BTC to be the evidence for the presence of nonequilibrium sorption effects.

Using the simplified method of estimation for radial flow, we fit Eq. (11) to the $^{131}$I BTC using $\hat{r}_{max} = 5.0$ m and estimated $\alpha_L = 6.4$ cm (MSE $= 1.67 \times 10^{-3}$). Then, keeping $\alpha_L$ fixed, we fit Eq. (11) to the $^{85}$Sr BTC and determined $\hat{r}_{max,Sr} = 1.48$ m (MSE $= 1.98 \times 10^{-3}$). This is in good agreement with experimental results where complete breakthrough of $^{85}$Sr was observed at $r = 0.66$ m, but no breakthrough of $^{85}$Sr was detected at $r = 2.06$ m [26]. Using Eq. (12), we estimated $R^*(^{85}\text{Sr}) = 11.4$, and rearranging Eq. (4) we determined $K_d = 2.33$ ml/g. Thus, reasonable agreement was found between values of $K_d$ determined from injection phase BTCs by Pickens et al. [26] and the $K_d$ value estimated from extraction phase BTCs using the simplified method of estimation presented in this study. In particular, the value of $K_d$ we determined (2.33 ml/g) matched closely the smallest value of $K_d$ (2.6 ml/g) reported by Pickens et al. [26], which was measured in a sublayer of the aquifer in which flow and transport were fastest. This agrees with the observation of preferential flow and transport that occurred during the simulation of a push–pull test conducted in a heterogeneous (layered) aquifer (Fig. 6(a)).

Moreover, a reasonable estimate of $K_d$ for $^{85}$Sr was obtained by our method despite the fact that Pickens et al. [26] observed effects of macrokinetics during their field test (effective dispersivity values for $^{85}$Sr were

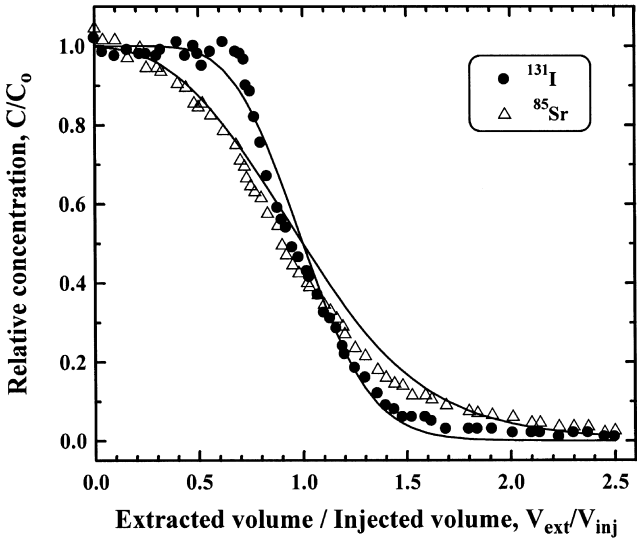


Fig. 7. Breakthrough curves for a tracer ($^{131}$I) and a sorbing solute ($^{85}$Sr) obtained by Pickens et al. [26] at the injection/extraction well during the extraction phase of a field push–pull test. Solid lines show fitted curves (Eq. (11)) employed to estimate $R$ using the simplified method of estimation.

typically a factor 2–5 larger than those obtained for $^{131}I$ during the field experiment). Apparently, nonideal flow conditions that cause macrodispersion and macrokinetics were mild enough to allow the successful application of our simplified method of estimation. Witness to this conclusion are both the fact that obtained values of MSR between measured and fitted BTCs were small and in the same range for tracer and sorbing solute, and that the point of coincidence of the $^{131}I$ and $^{85}Sr$ BTCs was near $V_{ext}/V_{inj} = 1$ (compare Figs. 2 and 7). Nonetheless, differences between the experimental data and the fitted BTCs (Fig. 7), particularly at late times, may be indicative of slight nonequilibrium sorption conditions during the experiment [10,21].

## 5. Summary and conclusions

The ability of the push–pull test to provide quantitative information on in situ solute retardation was evaluated. A simplified method for estimating retardation factors from extraction phase BTCs was developed for the case of radial flow based on a previously published analysis of variable dispersion during nonuniform flow [6]. Sensitivity analyses were conducted to evaluate the method's performance for a variety of simulated test conditions, including tests performed under both ideal and nonideal transport conditions. Finally, the method was applied to field data presented by Pickens et al. [26] to estimate the distribution coefficient of $^{85}Sr$ in a sandy aquifer.

Sensitivity analyses based on numerical simulations for tests conducted under ideal transport conditions in a physically and chemically homogeneous confined aquifer revealed errors $\leqslant 14\%$ between simulated and predicted values of $R$ for a wide range of aquifer and test conditions. The method was most sensitive to changes in aquifer dispersivity, whereas an uncertainty in aquifer effective porosity or thickness did not impede its successful use. In general, differences between simulated and predicted values of $R$ increased with increasing $R$. This was mainly attributed to the increased violation of an assumption (regarding the total travel distance of the solute front during a push–pull test) made in the development of the underlying approximate solutions to the transport equation.

Conversely, poor agreement between simulated and predicted values of $R$ was often found for simulations of push–pull tests conducted under nonideal transport conditions such as nonlinear equilibrium and linear nonequilibrium sorption, and in a test performed in a physically heterogeneous aquifer. Thus, the reader is cautioned against using this method to estimate retardation factors for either (1) very strongly or very slowly sorbing solutes, or (2) cases of severe aquifer heterogeneity (especially layering). Furthermore, no effort was made here to evaluate the potentially deleterious effects of macrokinetics (resulting from negatively correlated $K_d$ and $K$) on the method performance.

Nonetheless, when applied to a field data set presented by Pickens et al. [26], the method showed reasonable agreement with those authors' results in estimating the distribution coefficient of $^{85}Sr$ during transport in a sandy aquifer. This is particularly encouraging considering that nonideal transport conditions existed during the field experiment, i.e., the test was conducted in a heterogeneous aquifer that exhibited effects of macrokinetics. This indicates that push–pull tests and the simplified method of estimation may be used successfully for the in situ evaluation of solute sorption under certain test and aquifer conditions. However, further analyses, in particular additional application of this method to field data sets, will be required to better understand both the method's capabilities and limitations.

## Acknowledgements

This research was funded by the US Department of Energy, Environmental Management Science Program, Grant No. DE-FG07-96ER14721. Special thanks to Mart Oostrom and Mark White, Pacific Northwest National Laboratory, for providing the STOMP simulator. We would also like to thank the three anonymous reviewers and the journal editor, S.M. Hassanizadeh, for their helpful review comments.

## References

[1] Bear J. Hydraulics of groundwater. New York: McGraw-Hill; 1979.
[2] Chrysikopoulos CV, Kitanidis PK, Roberts PV. Generalized Taylor–Aris moment analysis of the transport of sorbing solutes through porous media with spatially peridiodic retardation factor. Transport in Porous Media 1992;7:163–85.
[3] Drever JI, McKee CR. The push–pull test. A method for evaluating formation adsorption parameters for predicting the environmental effects on in situ coal gasification and uranium recovery. In Situ 1980;4:181–206.
[4] Fetter CW. Contaminant hydrogeology. Upper Saddle River, NJ: Prentice-Hall; 1993.
[5] Gelhar LW. Stochastic subsurface hydrology. Englewood Cliffs, NJ: Prentice-Hall; 1993.
[6] Gelhar LW, Collins MA. General analysis of longitudinal dispersion in nonuniform flow. Water Resour Res 1971;7:1511–21.
[7] Gelhar LW, Welty C, Rehfeldt KR. A critical review of data on field-scale dispersion in aquifers. Water Resour Res 1992;28:1955–74.
[8] Gupta AD, Lake LW, Pope GA, Sepehrnoori K, King MJ. High-resolution monotonic schemes for reservoir fluid flow simulation. In Situ 1991;15:289–317.
[9] Haggerty R, Fleming SW, McKenna SA, STAMMT-R, Solute transport and multirate mass transfer in radial coordinates: a

FORTRAN for modeling and analyzing radial single-well and two-well tracer tests in formations exhibiting multiple rates of diffusive mass transfer, Version 1.01. SAND99-0164, 2000, Sandia National Laboratories, Albuquerque, New Mexico.

[10] Haggerty R, Fleming SW, Meigs LC, McKenna SA. Tracer tests in fractured dolomite: 2. Analysis of mass transfer in single-well injection–withdrawal tests. Water Resour Res 2000, in review.

[11] Haggerty R, Gorelick SM. Multiple-rate mass transfer for modeling diffusion and surface reactions in media with pore-scale heterogeneity. Water Resour Res 1995;31:2383–400.

[12] Haggerty R, Schroth MH, Istok JD. Simplified method of push–pull test data analysis for determining in situ reaction rate coefficients. Ground Water 1998;36:314–24.

[13] Hall SH, Luttrell SP, Cronin WE. A method for estimating effective porosity and ground-water velocity. Ground Water 1991;29:171–4.

[14] Harmon TC, Semprini L, Roberts PV. Simulating solute transport using laboratory-based sorption parameters. J Environ Eng 1992;118:666–89.

[15] Hoopes JA, Harleman DRF. Dispersion in radial flow from a recharge well. J Geophys Res 1967;72:3595–607.

[16] Istok JD, Field JA, Schroth MH, Sawyer TE, Humphrey MD. Laboratory and field investigation of surfactant sorption using single-well, push–pull tests. Ground Water 1999;37:589–98.

[17] Istok JD, Humphrey MD, Schroth MH, Hyman MR, O'Reilly KT. Single-well, push–pull test for in situ determination of microbial activities. Ground Water 1997;35:619–31.

[18] Lafolie F, Hayot C, Schweich D. Experiments on solute transport in aggregated porous media: are diffusions within aggregates and hydrodynamic dispersion independent. Transport in Porous Media 1997;29:281–307.

[19] Leap DI, Kaplan PG. A single-well tracing method for estimating regional advective velocity in a confined aquifer: theory and preliminary laboratory verification. Water Res 1988; 23:993–8.

[20] Mackay DM, Freyberg DL, Roberts PV, Cherry JA. A natural gradient experiment on solute transport in a sand aquifer 1. Approach and overview of plume movement. Water Resour Res 1986;22:2017–29.

[21] Meigs LC, Beauheim RL, McCord JT, Tsang YW, Haggerty R, Design, modelling, and current interpretations of the H-19 and H-11 tracer tests at the WIPP site, NEA/EC GEOTRAP Workshop. In: Field tracer experiments: role in the prediction of radionuclide migration. Nuclear Energy Agency, Paris, Cologne, Germany, 1997. p. 157–69.

[22] Mercado A, Underground water storage study: Recharge and mixing tests ant Yavne 20 well field. Technical Report No. 12, TAHAL – Water Planning for Israel Ltd., Tel Aviv, 1966.

[23] Miralles-Wilhelm F, Gelhar LW. Stochastic analysis of sorption macrokinetics in heterogeneous aquifers. Water Resour Res 1996;32:1541–9.

[24] Nichols WE, Aimo NJ, Oostrom M, White MD, STOMP: subsurface transport over multiple phases. Application guide. PNNL-11216, 1997, Pacific Northwest National Laboratory, Richland, WA.

[25] Pickens JF, Grisak GE. Scale-dependent dispersion in a stratified granular aquifer. Water Resour Res 1981;17:1191–211.

[26] Pickens JF, Jackson RE, Inch KJ, Merritt WF. Measurement of distribution coefficients using a radial injection dual-tracer test. Water Resour Res 1981;17:529–44.

[27] Ptak T, Schmid G. Dual-tracer transport experiments in a physically and chemically heterogeneous porous aquifer: effective transport parameters and spatial variability. J Hydrol 1996;183:117–38.

[28] Reinhard M, Shang S, Kitanidis PK, Orwin E, Hopkins GD, Lebron CA. In situ BTEX biotransformation under enhanced nitrate- and sulfate-reducing conditions. Environ Sci Technol 1997;31:28–36.

[29] Roberts PV, Goltz MN, Mackay DM. A natural gradient experiment on solute transport in a sand aquifer 3. Retardation estimates and mass balances for organic solutes. Water Resour Res 1986;22:2047–58.

[30] Sauty JP. Identification des paramètres du transport hydrodispersif dans les aquifères par interprétation de traçages en écoulement cylindrique convergent ou divergent. J Hydrol 1978;39:69–103.

[31] Schroth MH, Istok JD, Conner GT, Hyman MR, Haggerty R, O'Reilly KT. Spatial variability in in situ aerobic respiration and denitrification rates in a petroleum-contaminated aquifer. Ground Water 1998;36:924–37.

[32] Snodgrass MF, Kitanidis PK. A method to infer in situ reaction rates from push–pull experiments. Ground Water 1998;36:645–50.

[33] Trudell MR, Gillham RW, Cherry JA. An in situ study of the occurrence and rate of denitrification in a shallow unconfined sand aquifer. J Hydrol 1986;83:251–68.

[34] Valocchi AJ. Effect of radial flow on deviations from local equilibrium during sorbing solute transport through homogeneous soils. Water Resour Res 1986;22:1693–701.

[35] van Genuchten MT, Cleary RW, Movement of solutes in soil: computer-simulated and laboratory results. In: G.H. Bolt editor. Soil Chemistry, Physico-Chemical Models. New York: Elsevier; 1982, pp. 349–86.

[36] White MD, Oostrom M, STOMP: subsurface transport over multiple phases. Theory Guide. PNNL-11217, 1996, Pacific Northwest National Laboratory, Richland, WA.

[37] White MD, Oostrom M, STOMP: subsurface transport over multiple phases. User's Guide. PNNL-11218, 1996, Pacific Northwest National Laboratory, Richland, WA.